Effect of Material Properties and Processing Conditions on PP Film Casting

Kenneth Aniunoh and Graham Harrison
Department of Chemical and Biomolecular Engineering and
Center for Advanced Engineering Fibers and Films
Clemson University
Clemson, SC 29634-0909

Abstract

Film casting is a common industrial process used to produce polymeric films. The material properties and processing conditions have a significant impact on the process and the final thermal/mechanical properties. We experimentally investigate the impact of polymer molecular weight on the films. The effect of process conditions and post-processing steps like uniaxial stretching, on film strength, orientation and crystallinity is also studied. The measured velocity and temperature profiles are compared to model predictions.

Introduction

A significant fraction of the polymeric films used in various applications like food packaging and magnetic videotapes are produced via the film casting method. The film casting process consists of extruding a molten polymer material through a flat die. The extrudate/film is then cooled on a chill roll. The chill roll is run at higher velocities than the melt exits the die, thus stretching the polymer film and imparting some molecular orientation to the film. The cooled film from the chill roll is usually subjected to secondary processing steps depending on the end-use of the film [1]. The success of secondary processing steps such as biaxial stretching depends on the quality of the primary film.

Important process variables in film casting include the draw ratio, defined as the ratio of the velocity at the chill roll to the velocity at the die exit, and the air gap length [2]. The air gap length is the distance between the die exit and the point of contact between the film and the chill roll.

Changes in the polymer properties such as molecular weight (and hence viscosity) also affect the film formation process in the air gap [3,4]. For example, changing the polymer viscosity/molecular weight changes the resistance to flow in the region between the die exit and the chill roll and thus lead to variations in the film produced.

The film casting process as described here is 3-D, non-isothermal and extension dominated hence modeling this process is a complicated exercise. Obtaining valid numerical solutions to the models is aided by the availability of suitable experimental data. The experimental film casting data helps in the evaluation of process models and rheology assists in the selection of constitutive equations for the polymer stress as a function of the velocity gradients.

Some of the studies in literature geared towards predicting the film formation process in the web have employed isothermal Newtonian models [2,5], however, simulations that incorporate non-isothermal conditions and/or viscoelasticity [6-8] are physically more representative of the experimental conditions observed. Smith and Stolle [7] studied factors responsible for neck-in reduction and improved thickness uniformity. Dobroth and Erwin [9] showed that the primary cause of edge-beads is an edge stress effect.

In addition to the modeling efforts, there are some experimental reports in the literature. Canning et al. [10] made measurements of the film tension, velocity and width profiles. Lamberti et al. [11,12] investigated crystallinity and orientation in the film as a function of draw ratio. Acierno et al. [3] studied the temperature profiles in PET films. Seyfzadeh et al. [4] made point wise measurements of the velocity, width and temperature profiles for film casting of PET. Aniunoh and Harrison [13] studied the effects of draw ratio and die temperature on polypropylene film casting.

Biaxial stretching of polymer films produced from the film casting process helps impart molecular orientation to the film, thus improving the thermomechanical stability of the final film [14]. Elias et al [15] studied the effect of uniaxial/biaxial stretching on the morphology of polypropylene films. Adams et al [13] studied entanglement slippage in biaxially drawn PET films with the aim of extending a glass-rubber constitutive model to incorporate features such as stress-induced crystallization. Vigny et al [16] studied stretching of PET plates and determined that the strain induced crystallization proceeds at a faster rate with increasing strain rate.

The current work is geared toward understanding the effect of material properties and process conditions on the film casting process and thermomechanical properties of the final film. We focus on two polypropylene samples with different molecular weights/viscosities. The experimental results are compared to model predictions.

Experimental

The two polypropylene (PP) samples employed in this work are the X11291-37-1 (hereafter referred to as X171) and X11291-37-2 (X172) samples. Both samples were obtained from Basell Polyolefins and melt at Tm = 145 °C. Rheological characterization of the materials wasperformed using a TA Instruments ARES rheometer equipped with a 25 mm cone and plate geometry.

Figure 1 shows the complex viscosity * for the two PP samples at 220 ^{o}C. The X171 sample shows a higher plateau value of the complex viscosity, indicating that X171 has a higher molecular weight than X172. Both materials demonstrate shear thinning characteristics at high frequencies.

In Figure 2, we show a schematic of the domain of interest (e.g. the region between the die and the chill roll) in the film casting process. A 10.16 cm x 0.1 cm slit die and a 19.95 cm diameter chill roll are used for the film casting experiments presented in this work. The extruder throughput is maintained at 0.35 g/s while the air gap length is kept constant at 9 cm. Measurements were made throughout the polymer film both in the machine and the transverse directions. Increasing or decreasing the chill roll velocity leads to variations in the draw ratio.

Experimental measurements included film width, temperature and velocity as a function of position in the film. Temperature profiles were measured using infrared thermography (MIKRON infrared camera). Laser Doppler velocimetry (BETA LaserMike) was used to make point wise measurements of the velocity field in the web as a function of position in both the machine direction (MD) and the transverse direction (TD). A 0.03 % w/w seeding of TiO_2 particles was used to provide scattering centers for the velocity measurements. DMA experiments were performed on the X171 films (as produced from the film casting experiments) while DSC experiments were run using unstretched X171 film samples and X171 film samples that had been stretched (both uniaxially and biaxially) up to 4X the original length.

Model

The model makes use of the Giesekus constitutive equation and process modeling software developed by the Center for Advanced Engineering Fibers and Films at Clemson University. Details of the model development and boundary conditions are reported elsewhere [17].

Results and Discussion

Figure 3 shows the width profiles for the X171 and X172 samples at draw ratios of 6.5 and 12.8, and a die temperature of 220 ^{o}C. The width profiles show that both reducing the polymer viscosity and increasing draw ratio can cause an increase in the neck-in of the film. The increase in neck-in as the draw ratio is increased is due to mass conservation arguments. The observed dependence of neck-in on polymer viscosity is due to the restrictive influence of the edge beads [7]. Increasing the viscosity of the film increases the viscosity of the edge beads and thus improves the ability of the edge beads to restrict film neck-in. Thus, it is seen that the X172 sample displays a higher degree of neck-in at a constant draw ratio when compared to the X171 sample.

Figure 4 shows experimental centerline temperature profiles (as a function of distance from the die) for the X172 sample and and compares these results to model predictions. Experiments were conducted at a die temperature of 220 ^{o}C and draw ratio of 6.5. The model is seen to overpredict the temperature drop in the air-gap. This may be as a result of the heat transfer coefficients employed in the calculation.

Figure 5 shows experimental centerline velocity data for the X172 sample. The velocity increases with distance from the die. The velocity profile at DR = 6.5 is compared to model predictions. Although the model captures the qualitative shape of the experimental data, there is quantitative disagreement. The model prediction is consistent with the overprediction of the temperature in the air-gap.

Figure 6 shows a representative velocity map for the X171 and X172 samples at a die temperature of 220 ^{o}C and DR = 8.6. The machine direction component of velocity is reported as a function of both the transverse position in the web and distance from the die. At a given distance from the die, the maximum velocity is obtained in the central regions of the film.

This is primarily due to the technique used in the velocity measurement. The LDV method measures machine direction component of the velocity vector. Streamlines in the central regions of the film are parallel to the x-direction. However, near the film edges, the path of fluid elements results in both machine and transverse velocity components. This trend in the velocity map was also observed by Satoh et al. [8] and Sefzadeh et al. [4]. The velocity values are shown to differ for the X171 and X172 samples. This is primarily due to the different resistances to flow offered by the two samples by virtue of their different rheological properties.

Figure 7 shows the storage modulus, as obtained using a DMA instrument, as a function of temperature for a X171 film. The plot compares machine direction (MD) modulus values to the transverse direction (TD) values. The MD values are higher due to preferential molecular orientation in the MD [15]. Figure 8 shows DSC plots for unstretched and stretched (4X) X171 film. The difference in melting peaks is as a result of the existence of two different crystalline species in the stretched (and therefore oriented) film [15].

Conclusions

Film casting experiments were conducted using two different polypropylene samples in order to study the effects of polymer viscosity/molecular weight on film development in the region between the die exit and the chill roll. The film width, temperature profiles and draw direction velocity in the air gap were measured as a function of position within the web. The effect of uniaxial stretching on the produced cast film was also investigated.

Decreasing the polymer viscosity/molecular weight leads to an increase in neck-in at a constant draw ratio. Decreasing the polymer molecular weight decreases the polymer viscosity and this leads to a reduced restriction on neck-in by the edge beads.

Centerline temperature profiles show that the film cools more rapidly as the polymer viscosity/molecular weight increases. This is due to the improved heat transfer from the web resulting from the decreasing film thickness.

The centerline velocity increases with distance from the die exit. This is due to the acceleration of the polymer film in the air-gap. The velocity map also shows that a given distance from the die the maximum velocity occurs near the film centerline. This results from the extra die wall experienced by the film edges and the LDV technique used for measuring the velocity.

Post processing steps like uniaxial stretching are also seen to affect the film properties.

Acknowledgement

This work was supported by the Engineering Research Centers program of the National Science Foundation under award number EEC-9731680.

References

1. Baird, D. G. and D. I. Collias. (1995). Postdie Processing, *Polymer Processing: Principles and Design*, pp. 262, Butterworth-Heinemann, Boston.
2. Silagy, D., Y. Demay, and J. F. Agassant. (1999). Numerical Simulation of the Film Casting Process, *International Journal for Numerical Methods in Fluids*, 30: 1-18.
3. Acierno, D. and L. Di Maio. (2000). Film Casting of Polyethylene Terephthalate: Experiments and Model Comparisons, *Polymer Engineering and Science*, 40(1): 108-117.
4. Seyfzadeh , B., C. D. Carlson and G. M. Harrison. (2005). Experimental Studies on the Development of a Cast Film, *Polymer Engineering and Science*, 45: 443-450.
5. Yeow, Y. L.. (1974). On the Stability of Extending Films: A Model for the Film Casting Process, *Journal of Fluid Mechanics*, 66(3): 613-622.
6. Alaie, S. M. and T. C. Papanastasiou. (1991). Film Casting of Viscoelastic Liquid, *Polymer Engineering and Science*, 31(2): 67-75.
7. Smith, S. and D. Stolle. (2000). Nonisothermal Two-Dimensional Film Casting of a Viscous Polymer, *Polymer Engineering and Science*, 40(8): 1870-1877.
8. Satoh, N., H. Tomiyama and T. Kajiwara. (2001). Viscoelastic Simulation of Film Casting Process for a Polymer Melt, *Polymer Engineering and Science*, 41(9): 1564-1579.

9. Dobroth, T. and L. Erwin. (1986). Causes of Edge Beads in Cast Films, *Polymer Engineering and Science*, 26(7): 462-467.
10. Canning, K., B. Bian and A. Co. (2001). Film Casting of a Low Density Polyethylene Melt, *Journal of Reinforced Plastics and Composites*, 20(5): 366-376.
11. Lamberti, G., V. Brucato and G. Titomanlio. (2002). Orientation and Crystallinity in Film Casting of Polypropylene, *Journal of Applied Polymer Science*, 84: 1981-1992.
12. Lamberti, G. and V. Brucato. (2003). Real-Time Orientation and Crystallinity Measurements during the Isotactic Polypropylene Film-Casting Process, *Journal of Polymer Science: Part B: Polymer Physics*, 41: 998-1008.
13. Aniunoh, K. and G. M. Harrison. Experimental Investigation of Film Formation: Film Casting, *Journal of Plastic Film and Sheeting (in print).*
14. Adams, A. M., C. P. Buckley and D. P. Jones. (2000). Biaxial hot drawing of poly(ethylene terephthalate): measurements and modeling of strain-stiffening, *Polymer,* 41: 771-786.
15. Elias, M. B., R. Machado and S. V. Canevarolo. (2000). Thermal and dynamic-mechanical characterization of uni-and biaxially oriented polypropylene films, *Journal of Thermal Analysis and Calorimetry,* 59: 143-155.
16. Vigny, M., A. Aubert, J. M. Hiver, M. Aboulfaraj and C. G'Sell. (1999). Constitutive Viscoplastic Behavior of Amorphous PET during Plane-Strain Tensile Stretching, *Polymer Engineering ad Science,* 39(12): 2366-2376.
17. Cox, C. and J. B. von Oehsen. (2007). A Finite Element Model of non-Isothermal Viscoelastic Flow in the Cast Film Process. *SPE-ANTEC 2007 proceedings.*

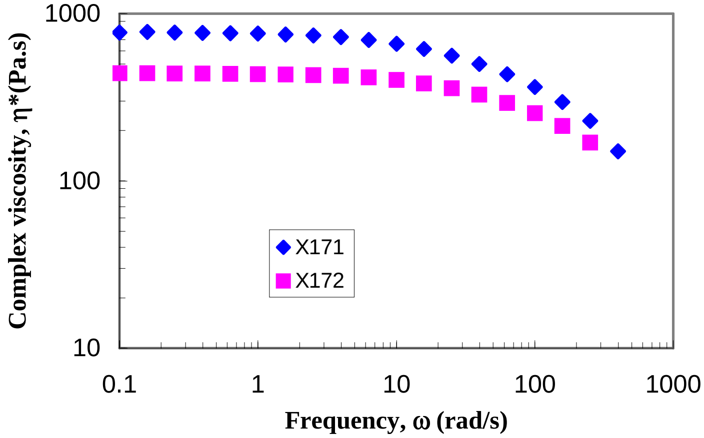

Fig. 1. Complex viscosity for Polypropylene samples at 220°C.

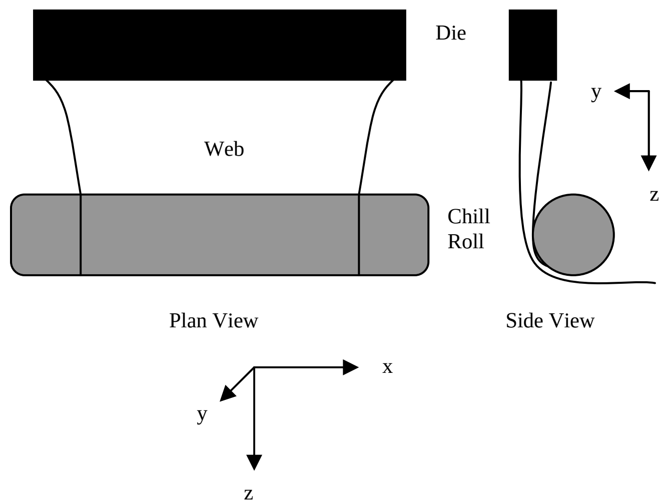

Fig. 2. Film casting Schematic

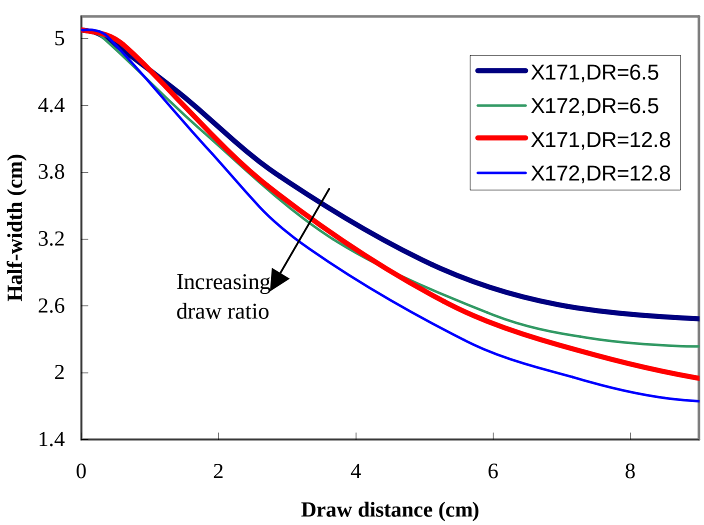

Fig. 3. Width profiles for polypropylene samples as a function of draw ratio at die temperature of 220 °C

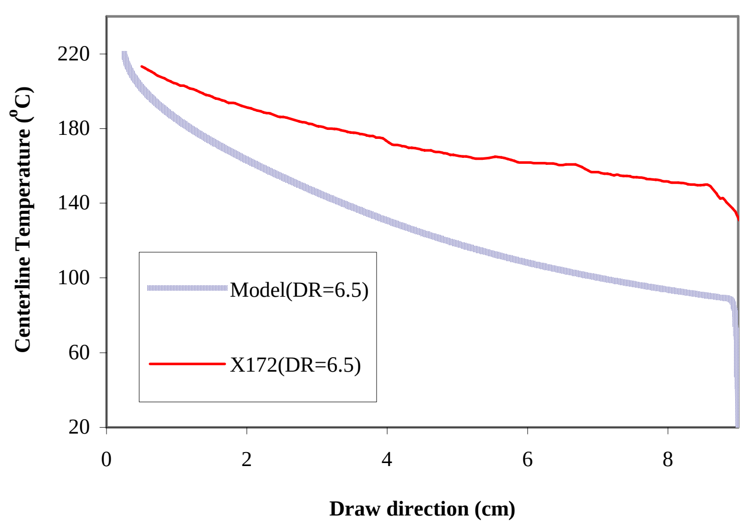

Fig. 4. Comparison of experimental data with model predictions for centerline temperature profile for X172 at die temperature of 220 °C and draw ratio of 6.5.

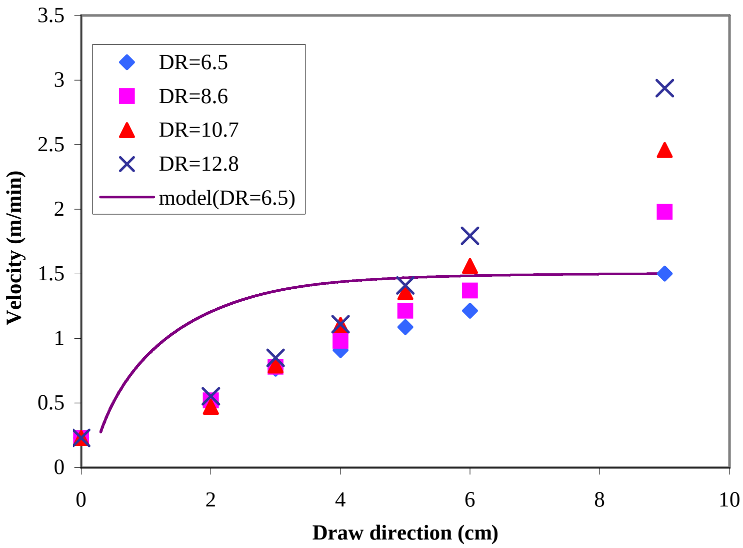

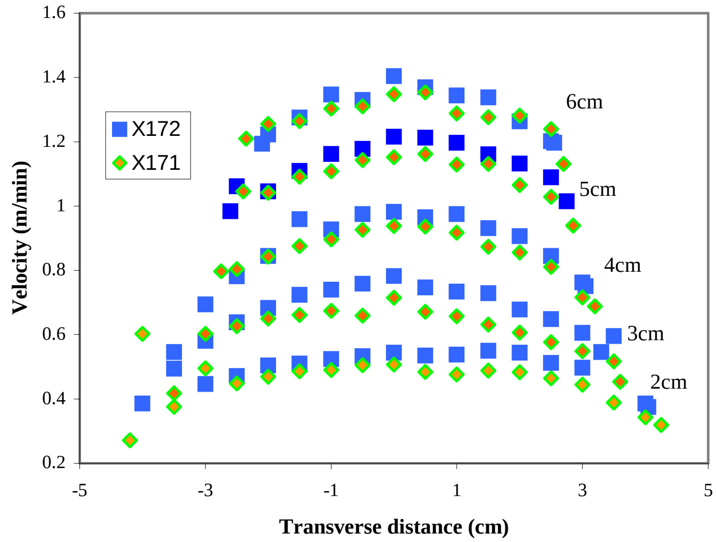

Fig. 5. Centerline velocity profiles for X172 sample at a die temperature of 220 °C. The plot also shows the model prediction for draw ratio of 6.5

Fig. 6. Velocity map for x171 and X172 films at DR = 8.6.

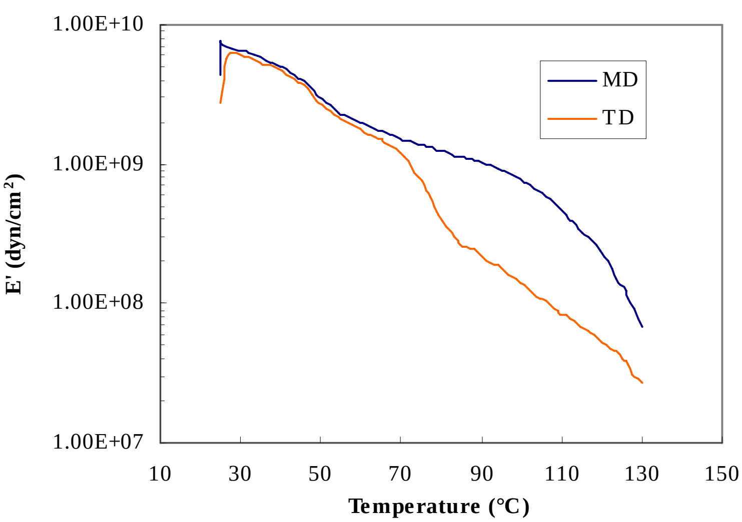

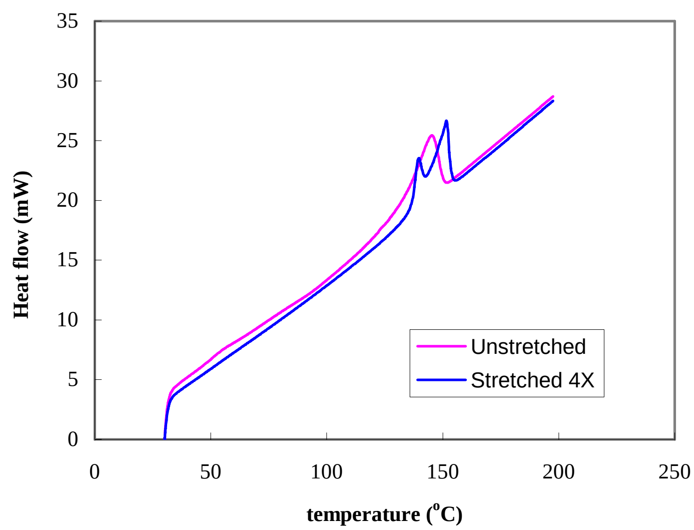

Fig. 7. DMA plot of storage modulus for X171 as function of temperature. Molecular orientation in the machine direction is seen as difference I modulus between the machine direction (MD) and transverse direction (TD).

Fig. 8. DSC plot showing difference in melting peaks for stretched and unstretched film samples for the X171 sample.

Keywords

Cast film; LDV; neck-in; extensional flow

www.tappiplace.org

PLACE

POLYMERS • LAMINATIONS • ADHESIVES • COATINGS • EXTRUSIONS

2007 PLACE Conference

September 16-20

St Louis, MO

Effect of Material Properties and Processing Conditions on PP Film Casting

Kenneth Aniunoh and Graham Harrison

Presented by:
Kenneth Aniunoh Title
Center for Advanced Engineering Fibers and Films
Clemson University

Outline

- **Introduction**
- **Motivation and Objectives**
- **Materials and Experimental Equipment**
- **Experimental Results**
- **Modeling**
- **Conclusions**

Introduction

- Film casting is used in the production of polymeric films
- Typical applications include
  - Magnetic videotapes
  - Plastic bags
  - Food packaging
- Process is
  - Non-isothermal
  - Three-dimensional
  - Extension dominated

Introduction

- **Film casting process consists of several distinct operations**
  - **Extruder**
  - **Extruding molten material through a nominally flat die**
  - **Stretching of the polymer between the die and the chill roll**
    - **Extensional flow**
    - **Non-isothermal**
    - **Three-dimensional**
  - **Cooling at the chill roll**
  - **Subsequent biaxial stretching**

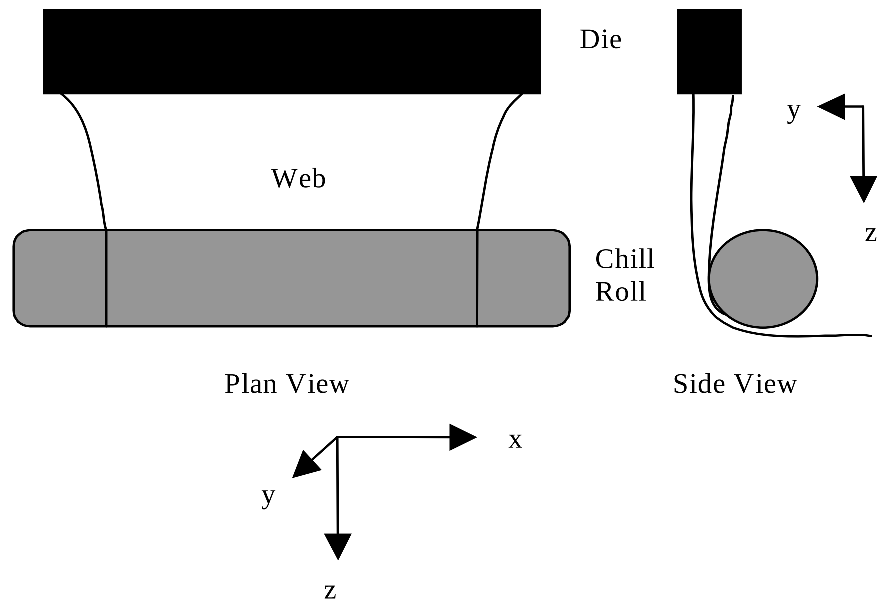

Fig. 1. Schematic of the Film Casting apparatus

Introduction

- **Variables that may be manipulated**
  - **Draw Ratio – ratio of chill roll velocity to melt velocity at the die exit**
  - **Die and Chill roll temperature**
  - **Air gap – distance from die exit to chill roll**
  - **Polymer type**
    - **Architecture**
    - **Molecular weight**
    - **Viscosity**

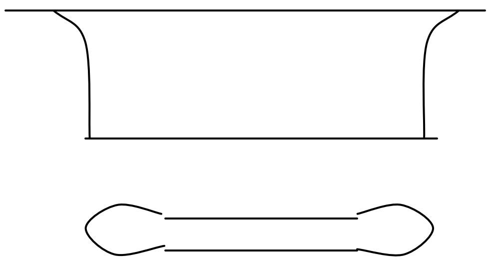

- **Characteristics of cast films**
  - **Neck-in – decrease in film width due to mass conservation**
  - **Edge beads – film is thicker at the edges**
  - **Draw Resonance – occurs at high draw ratios and is manifested as a process instability characterized by periodic fluctuations in film thickness**

Motivation and Objectives

- **Motivation**
  - **Quality of the final film depends on the film formation between the die and the chill roll**
  - **Quantitative fundamental understanding of the cast film process**
  - **Modeling of complex 3D, non-isothermal, extension dominated flow geometry**
  - **Limited experimental data**
- **Primary objectives of this work are**
  - **To understand how material properties and process conditions impact film formation**
  - **To provide comprehensive experimental data for model verification as a function of position**

Measurements in this work

- Velocity, width and temperature profiles
  - Transverse and draw directions
  - Varying die temperature, draw ratio and air-gap
  - Effect of material properties
- Film properties
  - Effect of processing

Materials and Experimental Equipment

- **Polypropylene**
  - **X11291-37-1 (X171), X1129-37-2 (X172), T_m = 146 °C**
  - **Profax PH 835, T_m = 168 °C**
- **Experimental apparatus**
  - **Rheology**
    - **TA Instruments ARES rheometer**
      - **Dynamic**
      - **Transient elongational**
    - **ACER capillary rheometer**
  - **Film Casting apparatus**
    - **Lab Scale**
    - **LDV (BETA LaserMike)**
    - **IR camera (MIKRON)**

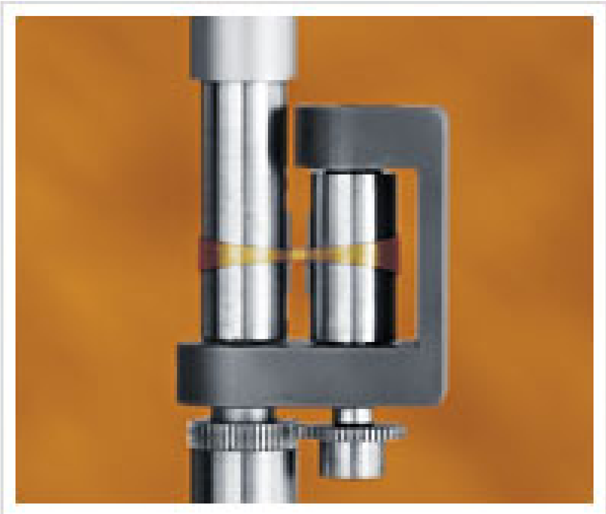

Extensional viscosity fixture

Experimental Equipment

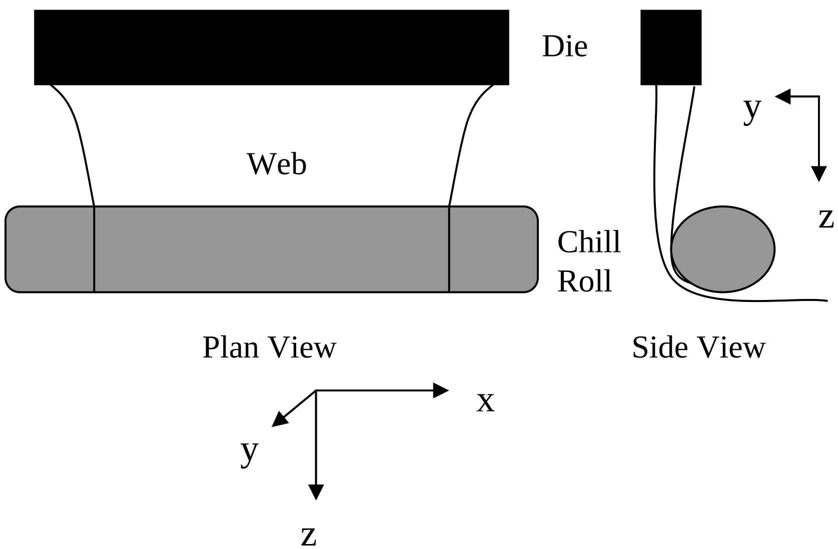

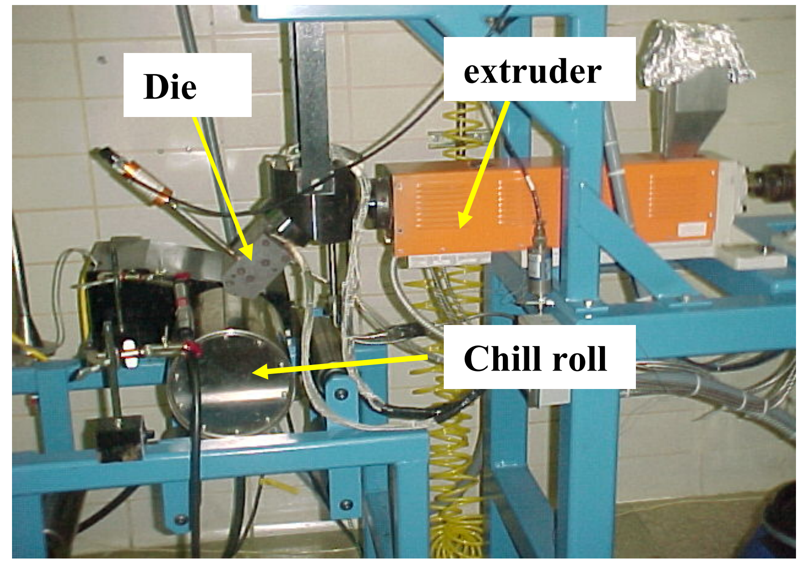

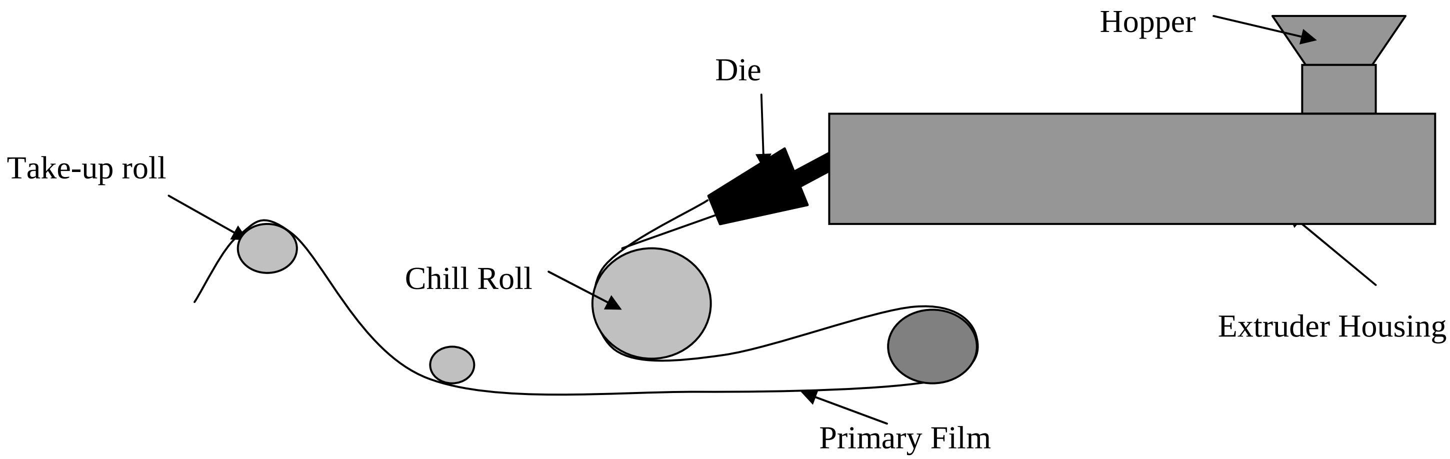

Experimental Results (Rheology)

- **Shear Rheology**

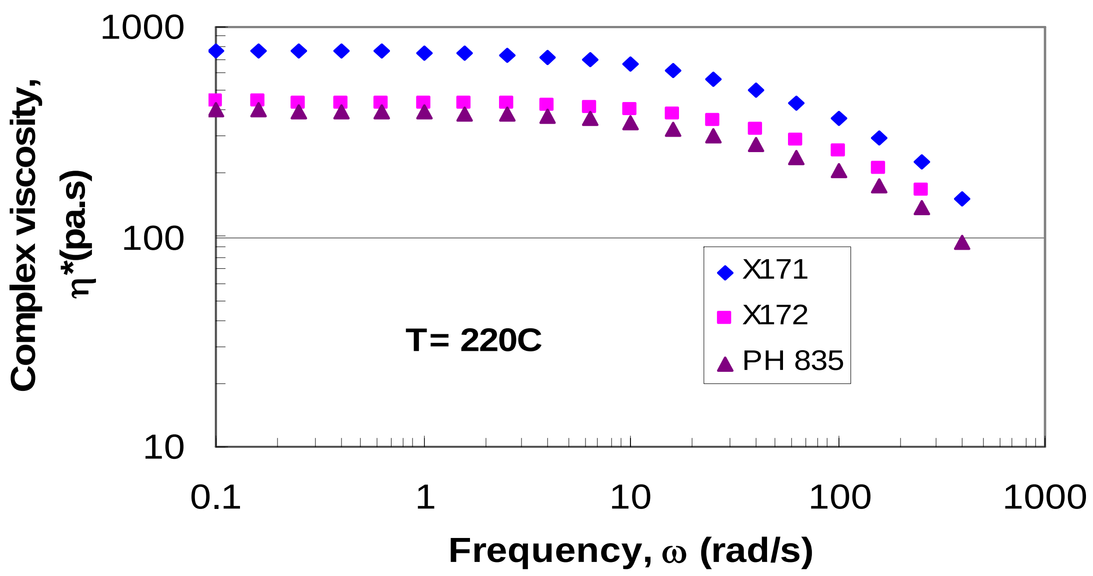

- **T = 220 °C, PH 835, X171 and X172**
- **Rheological properties are material dependent**

Experimental Results (Width)

- **Width profiles**

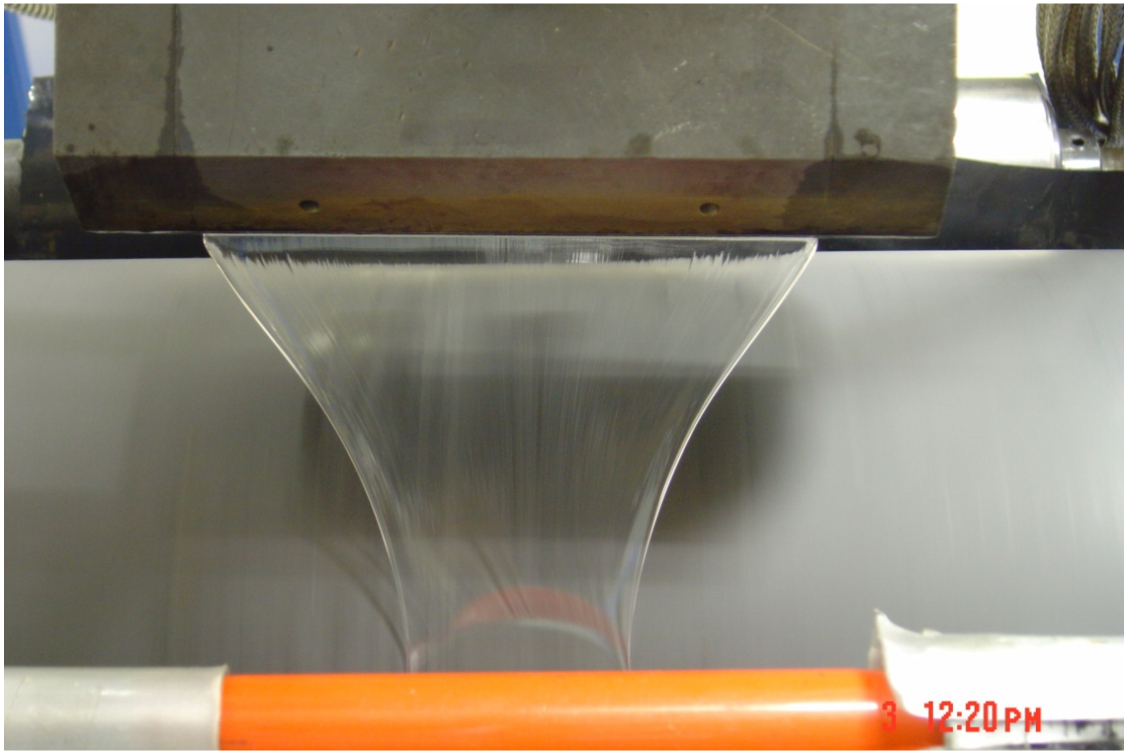

  - **Width profile obtained from digital pictures**
  - **Edge-beads**
  - **Neck-in (10.16 cm to 3.8 cm)**

Experimental Results (Width)

- **Effect of air-gap length and material on width profile**

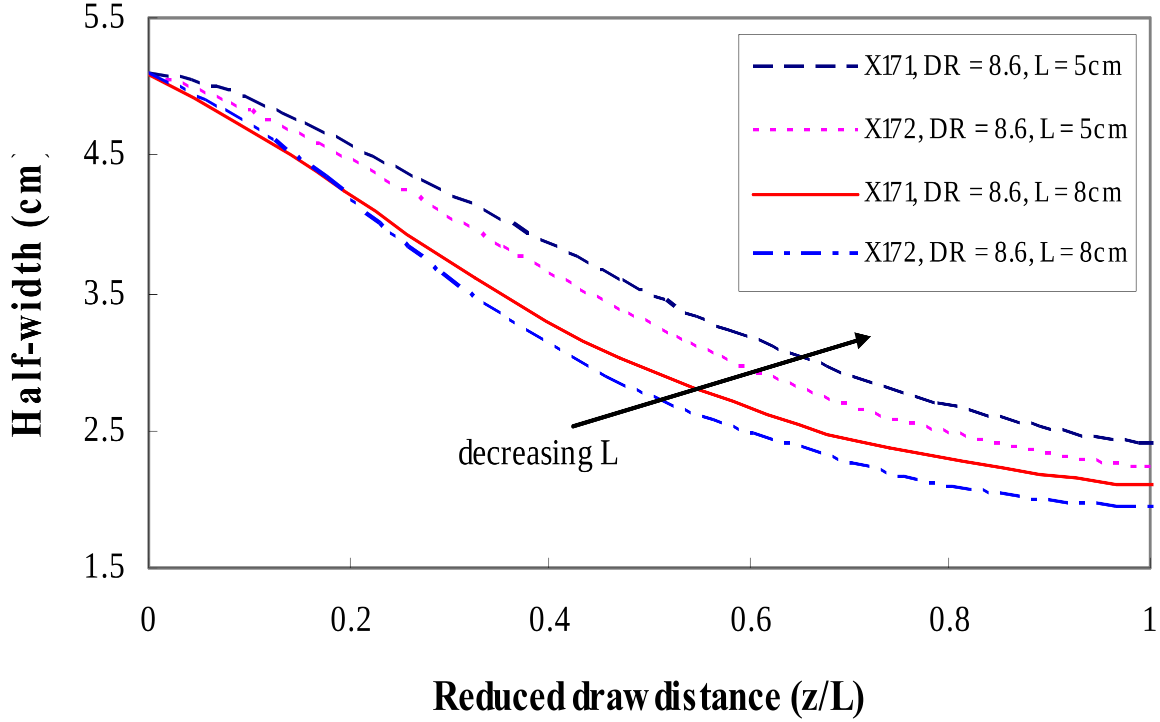

- **T_{die} = 220 °C, L= 8 cm and 5 cm**
- **Neck-in increases with increasing air-gap, and decreasing polymer viscosity**

Experimental Results (Width)

- **Effect of die temperature on width profile**

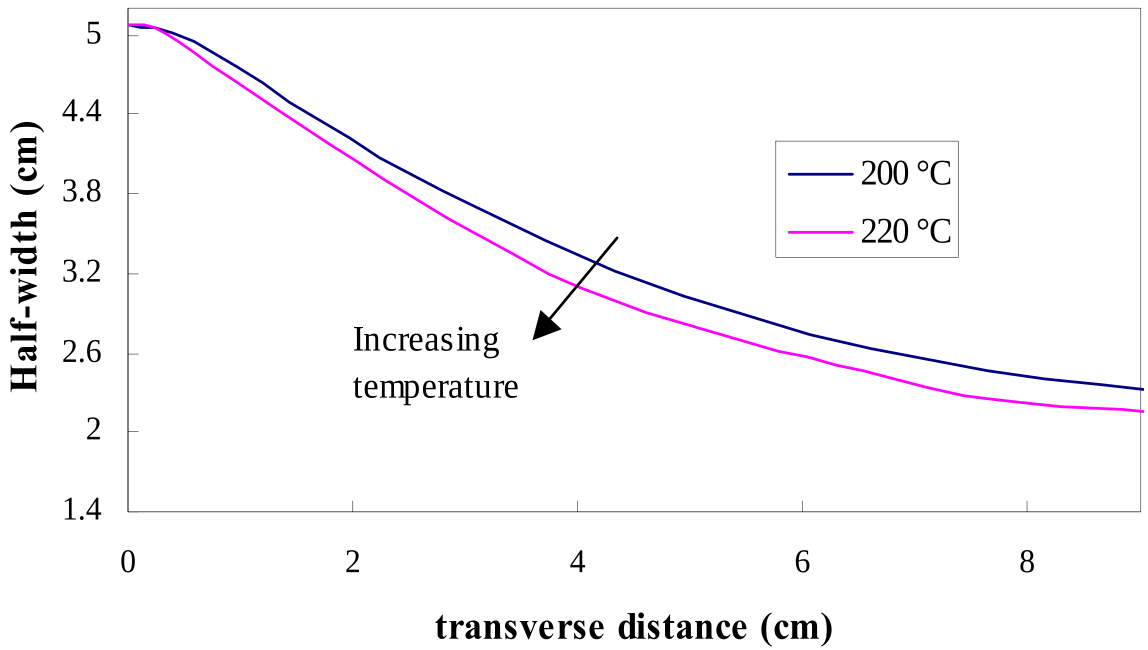

- **DR= 8.6, L = 9 cm, X171**
- **8% change from 200 °C to 220 °C**
- **Due to temperature effects on viscosity**

Experimental Results (Thickness profile)

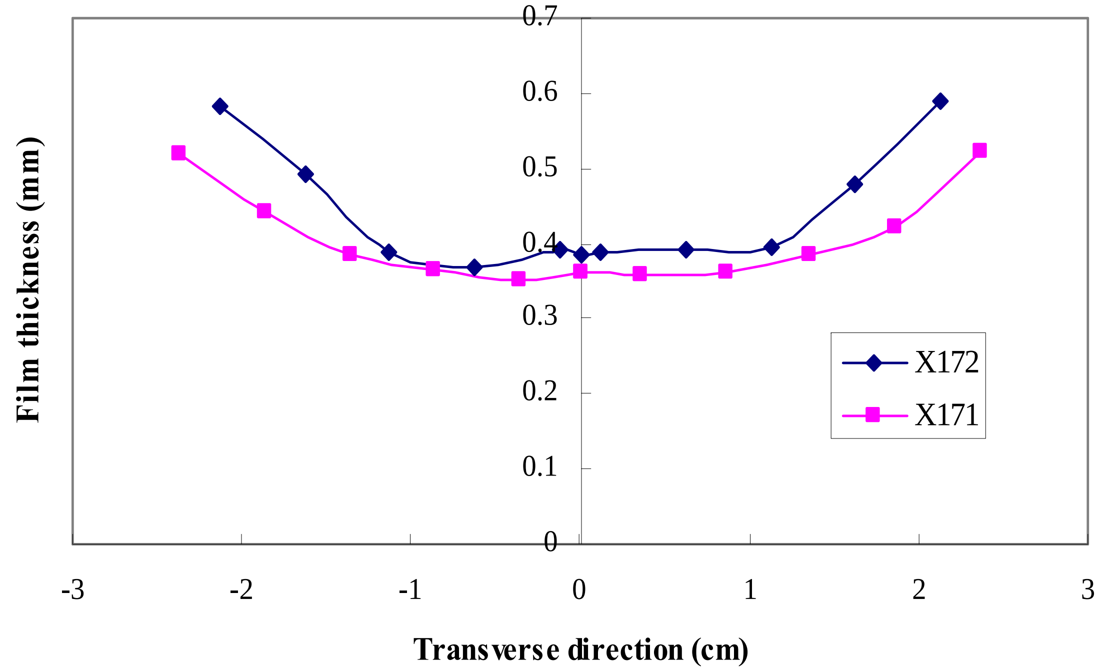

- **DR = 6.5, T_{die} = 220 °C**
- **X171 film experiences less neck-in than the X172 film**
- **X172 film is thicker than the X171 film**

Experimental results (Temperature)

- **Temperature profiles**

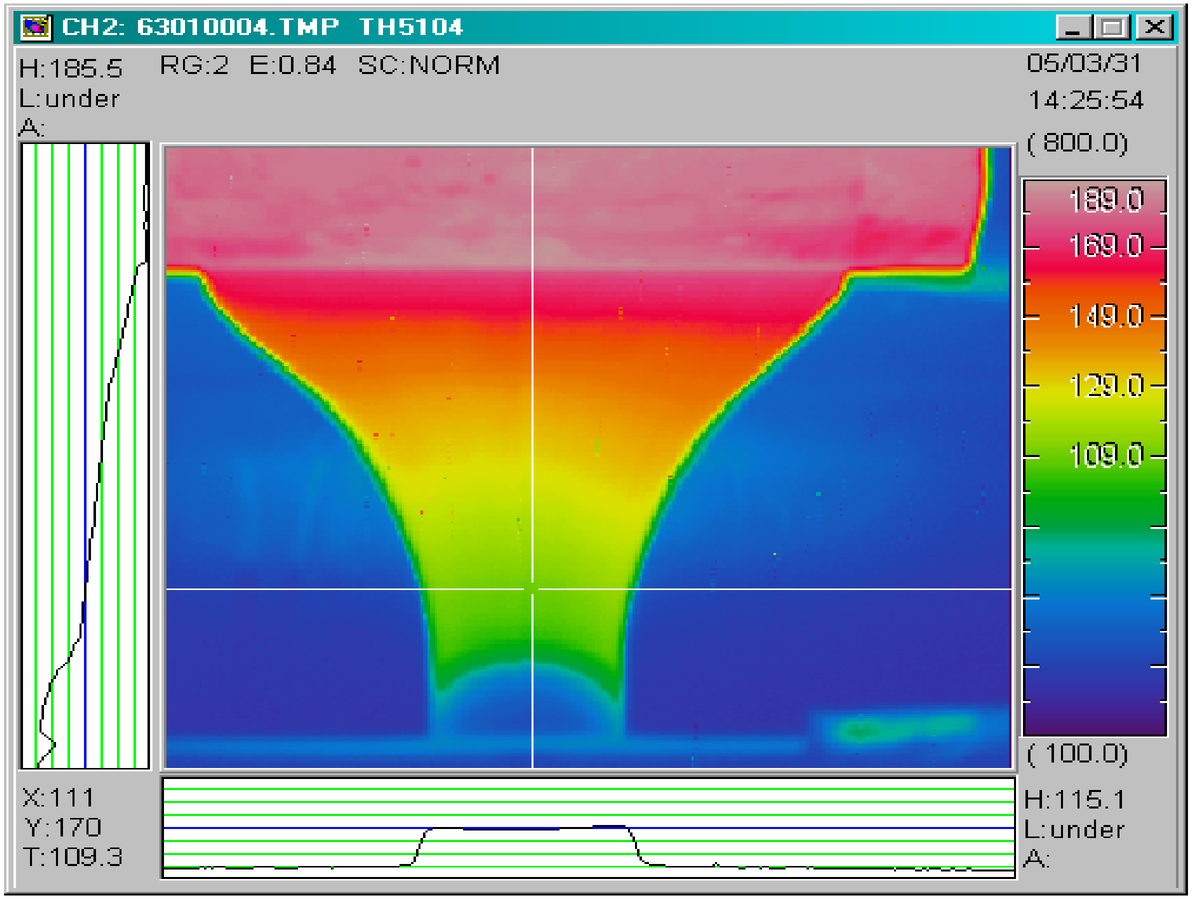

  - **Infrared camera is used for obtaining the temperature profiles.**

Experimental results (Temperature)

- **Effect of air-gap length and material on temperature profile**

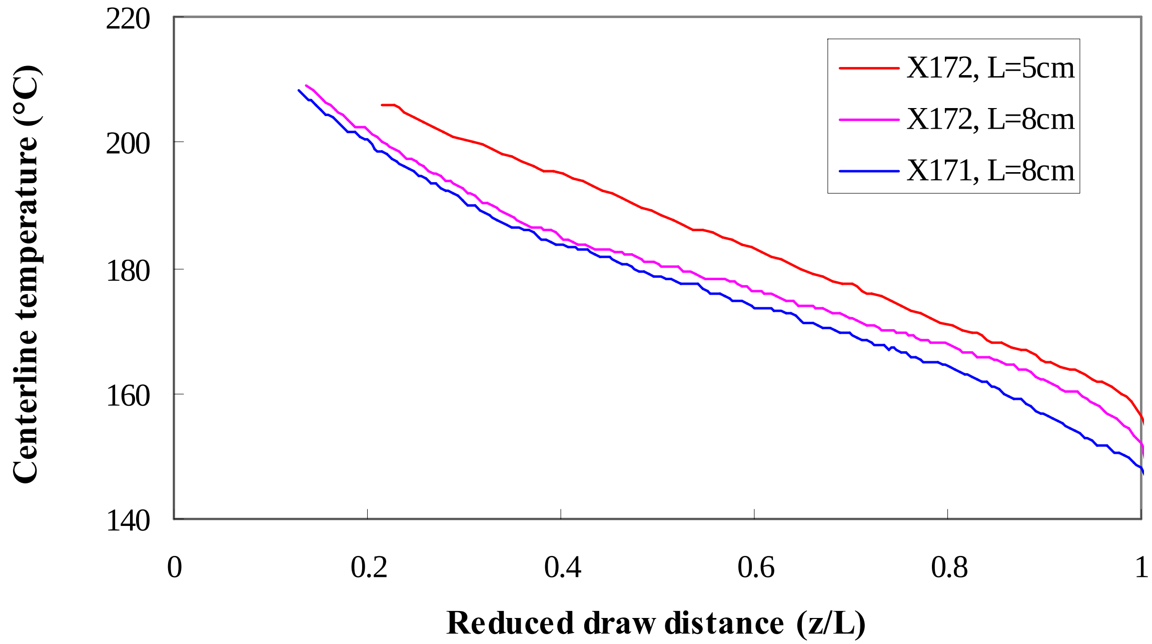

- **Centerline temperature profile, T_{die} = 220 °C, L = 5 and 8 cm, DR = 8.6**
- **Temperature decreases with distance from die**
- **X171 film cools more rapidly than the X172 film (6 °C)**
- **Due to difference in film thickness**

Experimental results (Temperature)

- **Effect of draw ratio on temperature profile**

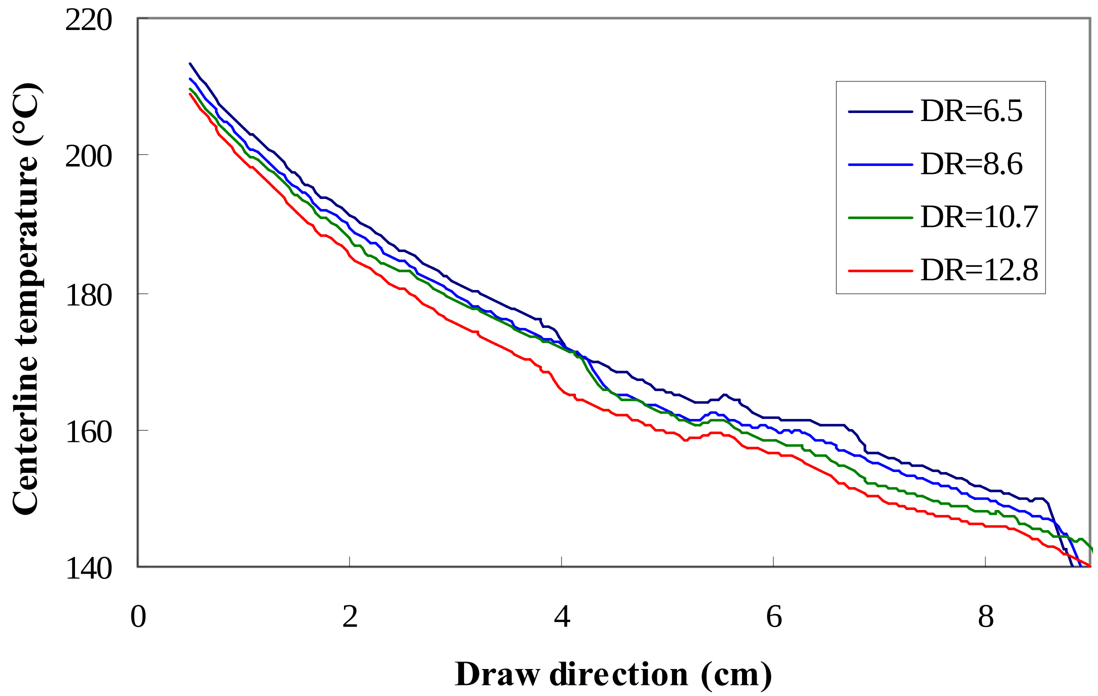

- **Draw ratio varied by manipulating the throughput**
- **T_{die} = 220 °C, L = 9 cm, X172**
- **Film cools more rapidly with increasing draw ratio**
- **Supports conduction being significant in heat transfer**

Experimental results (Velocity)

- **Centerline velocity profile**

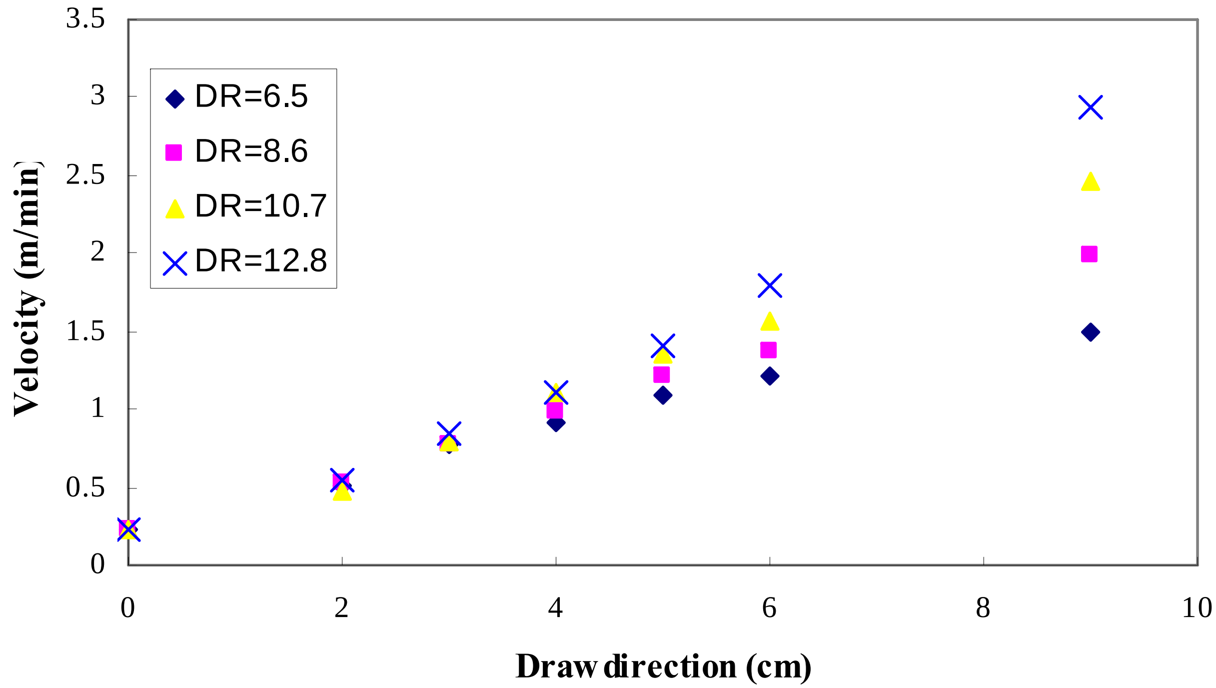

  - **T_{die} = 220 °C, L = 9 cm, X172**
  - **PP is seeded with 0.03% w/w of TiO_2 particles (10–45 microns)**
  - **TiO_2 particles provide scattering sites for laser beams (LDV)**
  - **Velocity increases with distance from die**

Experimental results (Velocity)

- **Centerline Strain rates**

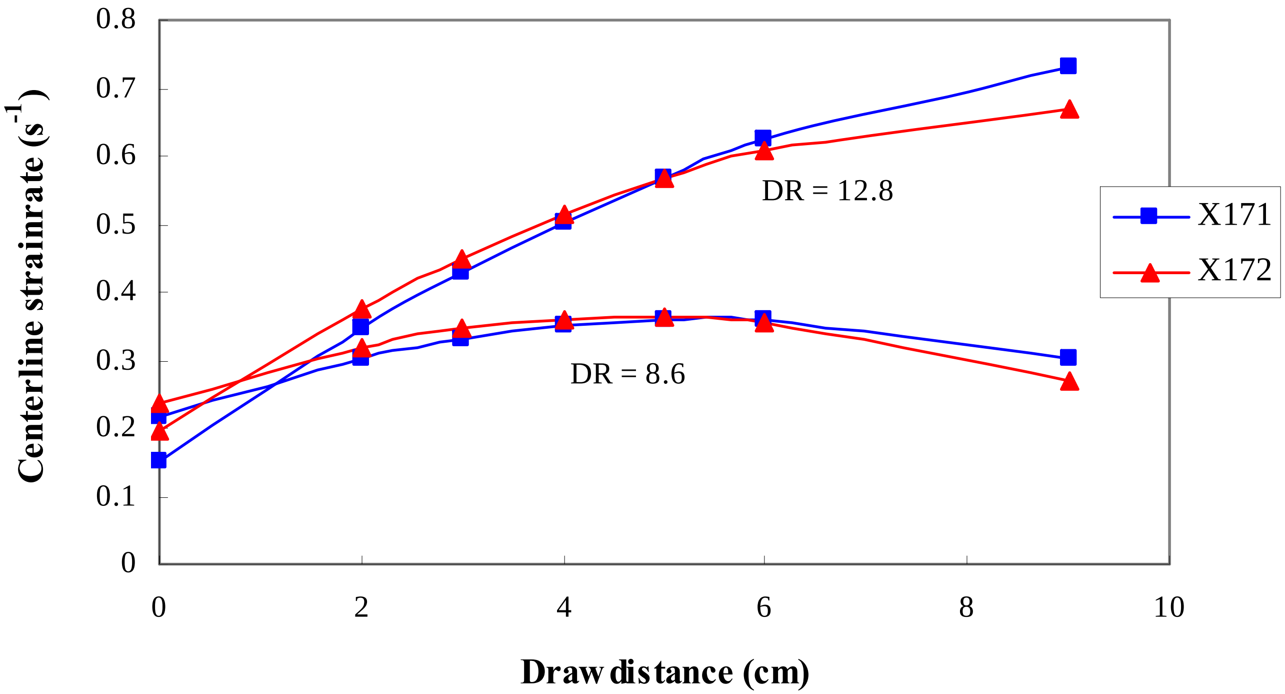

  - **Increase in strain rate (dv_z/dz) near the die**
  - **At low DR strain rate decreases near the chill roll.**
  - **Due to variation in film tension with increase in DR**

Experimental results (Velocity)

- **Velocity profiles as function of transverse position**

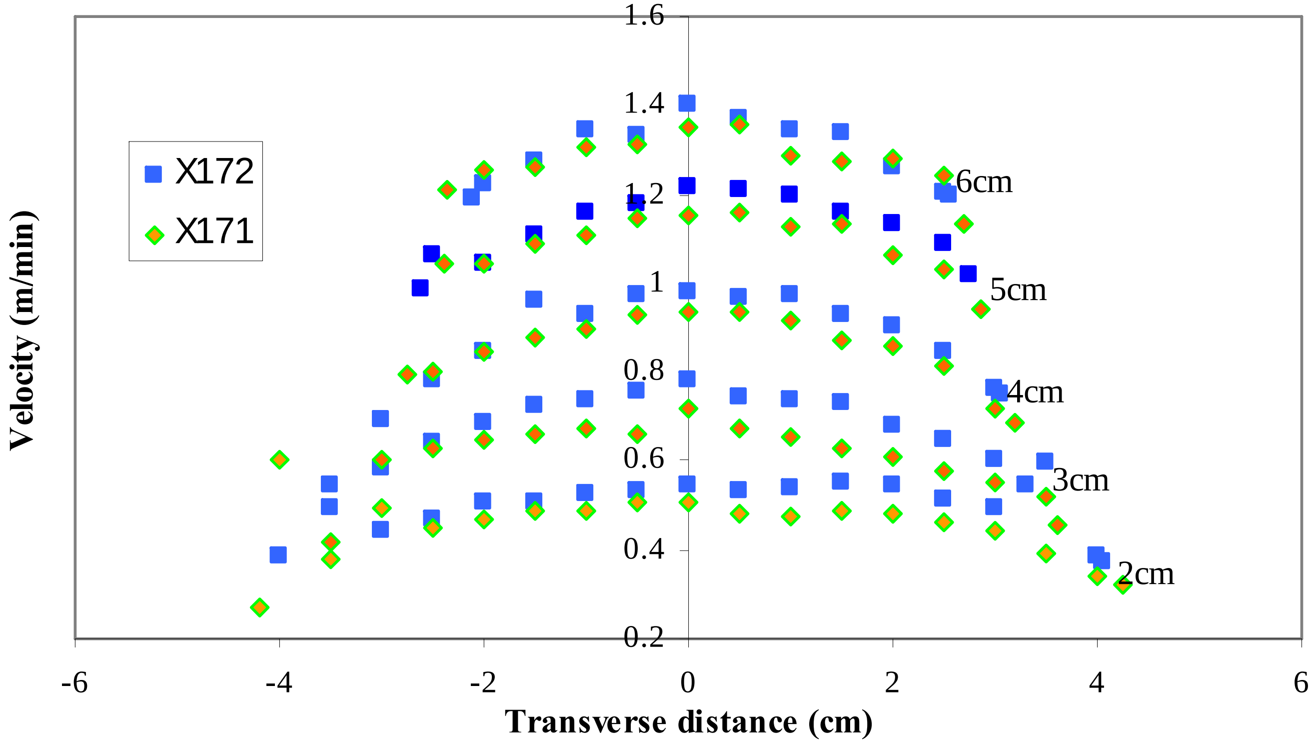

  - **T_{die} = 220 °C, L = 9 cm, DR = 8.6**
  - **Velocity decreases toward film edge**

Experimental results (Transverse direction velocity)

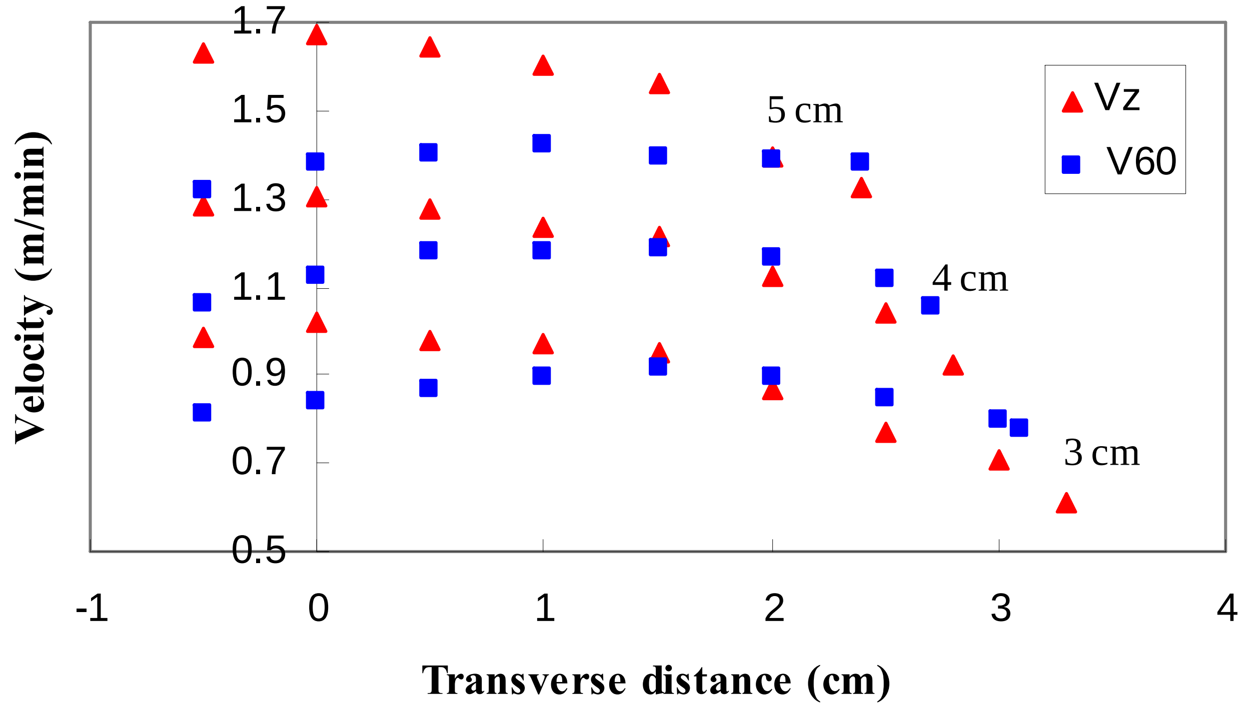

- **X172, T_{die} = 220 °C, L = 8 cm, DR = 12.8**
- **Velocity components along the z-axis and at 60° to the x-axis**

Experimental results (Transverse direction velocity)

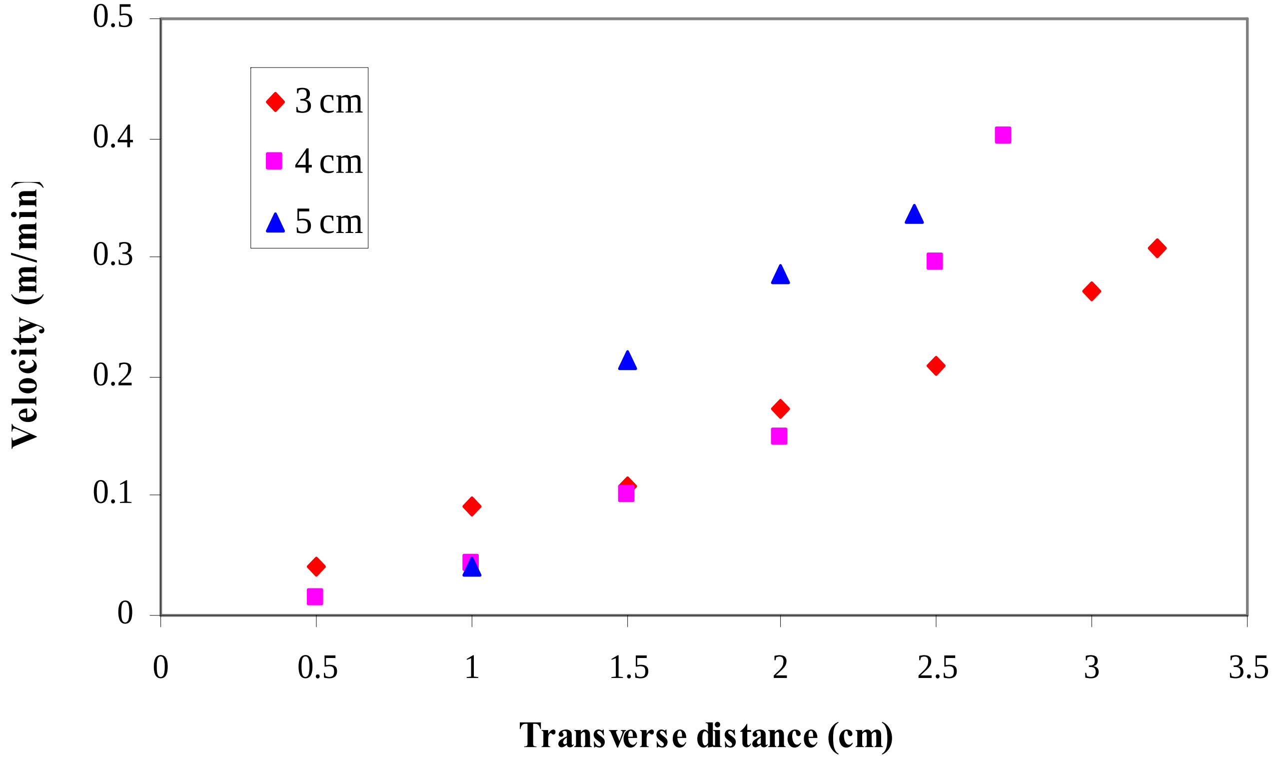

- **X172, T_{die} = 220 °C, L = 8 cm, DR = 8.6**
- **v_x calculated from v_z and v_{60}**
- **Velocity decreases from edge to the centerline**

Experimental results (velocity vector)

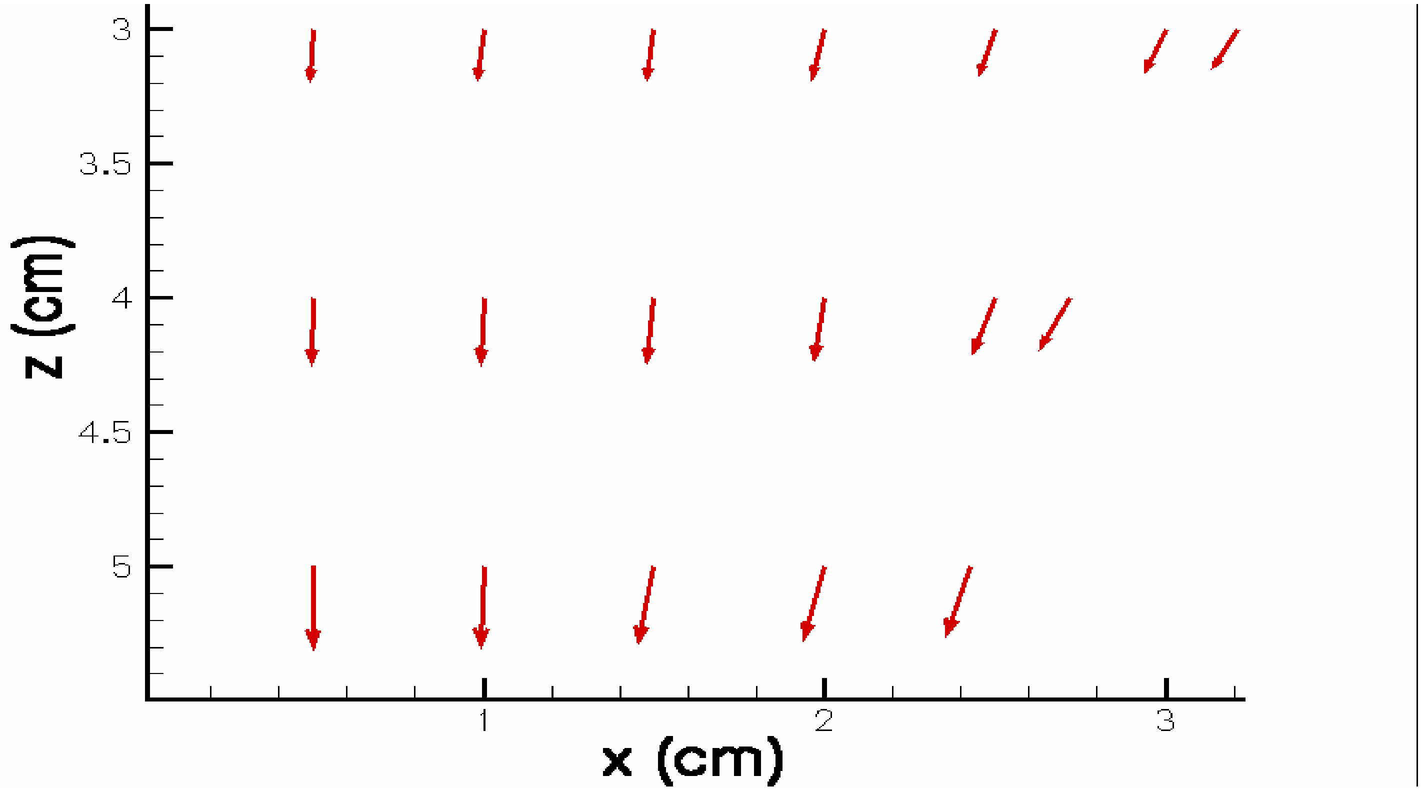

- X172, L = 8cm, T_{die} = 220 °C, DR = 8.6
- Direction of the velocity vector

Biaxial and Uniaxial Stretching

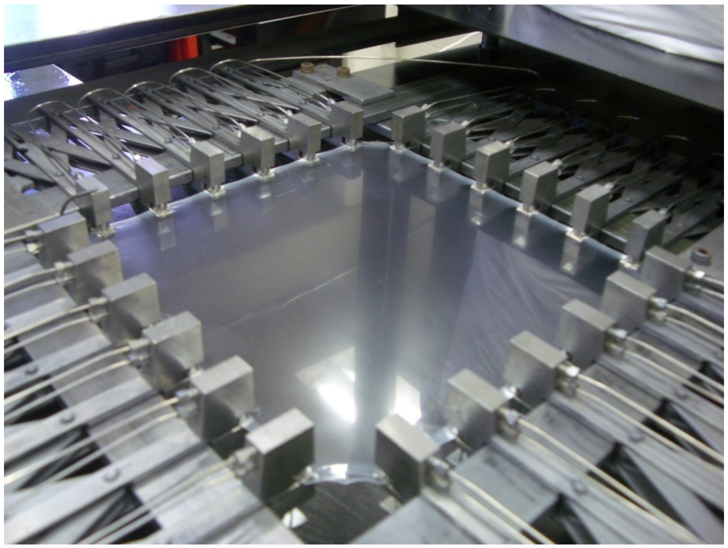

- Uniaxial Stress-Strain response
- Biaxial Stress-Strain response
- Minimum Gauge Length 50 mm
- Maximum Gauge Length 250 mm
- Compressed Nitrogen Piston Grips

Experimental results (WAXD)

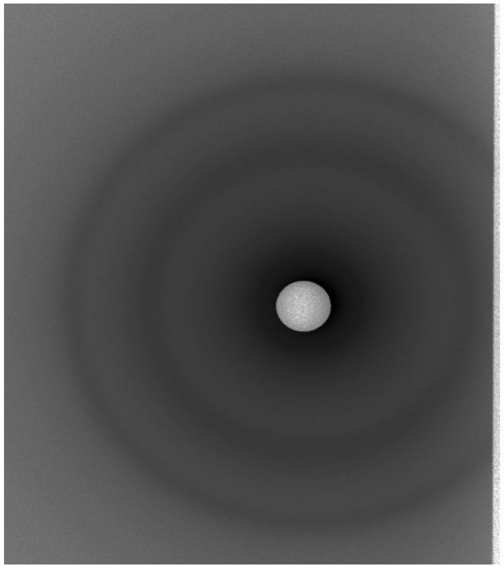

(a)

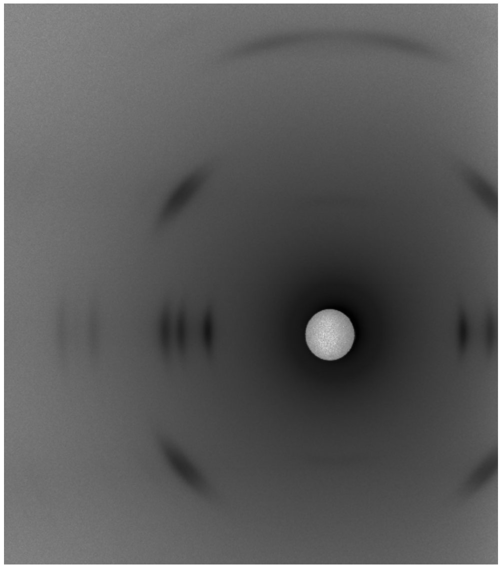

(b)

- **X171, DR = 8.6, T_{die} = 220 °C**
- **(a) Unstretched film (b) Stretched film**

Experimental results (WAXD)

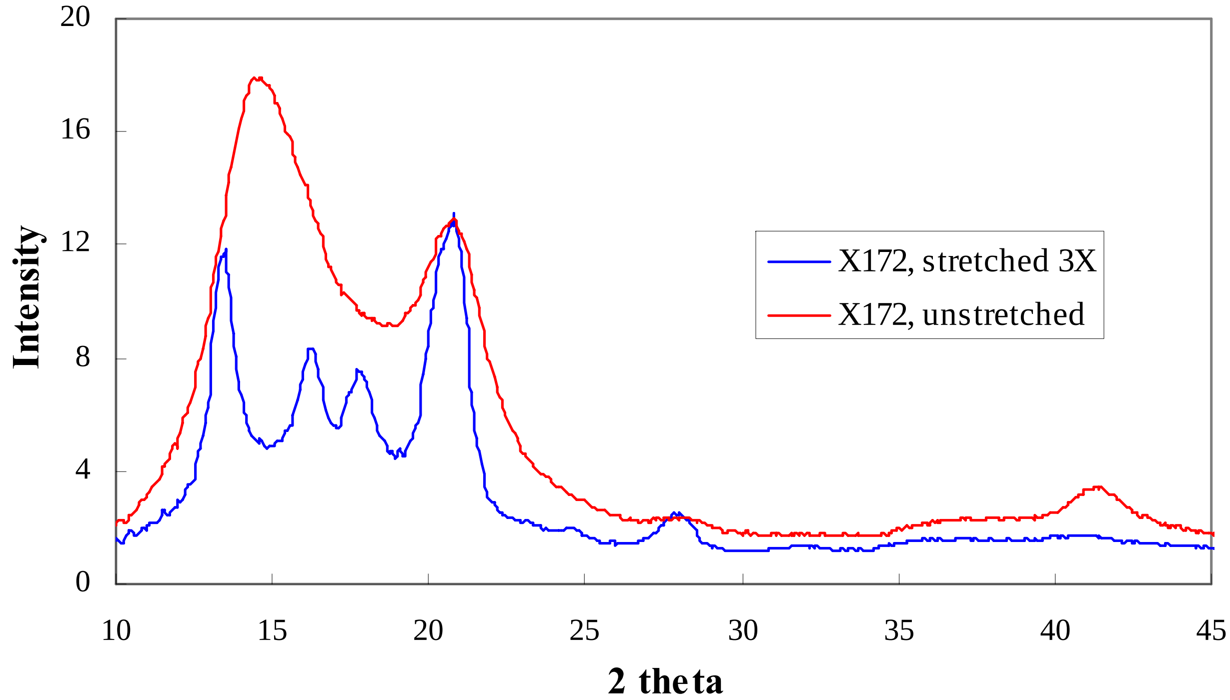

- **X172, DR = 8.6, T_{die} = 200 °C**
- **Unstretched sample crystallizes in mesomorphic form**
- **Stretching causes reorganization of crystals into α-form**

Experimental results (Film DSC)

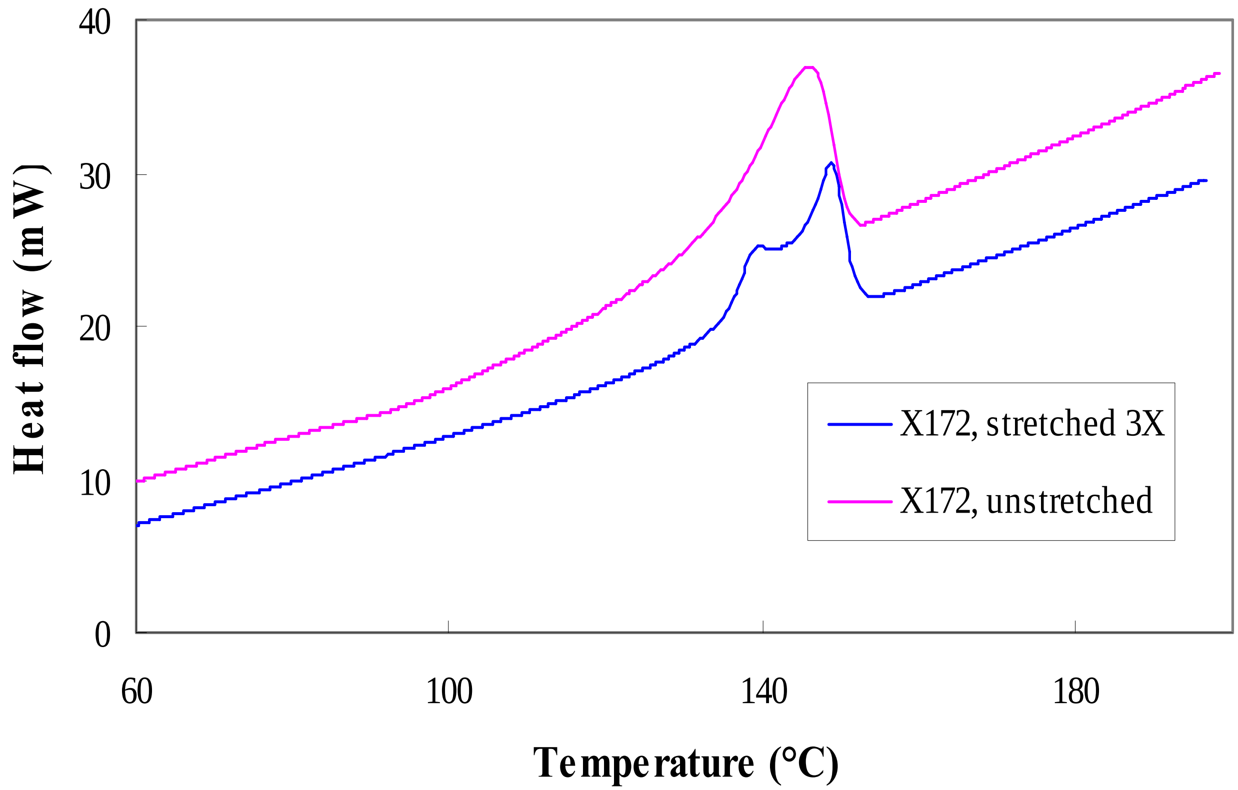

- **X172, DR = 8.6, T_{die} = 200 °C**
- **Stretching changes the crystalline morphology**

Experimental results (Film properties)

Draw Ratio	ΔH_m (J/g)	Modulus (MPa)
8.6	72.2	720
12.8	77.6	789.4
8.6, 3X	91.4	901.3

- **X172, L=5cm, T_{die} = 200 °C**
- **Increasing draw ratio increases crystallinity and modulus**
- **Stretching increases orientation, crystallinity and modulus**

Experimental results (DMA)

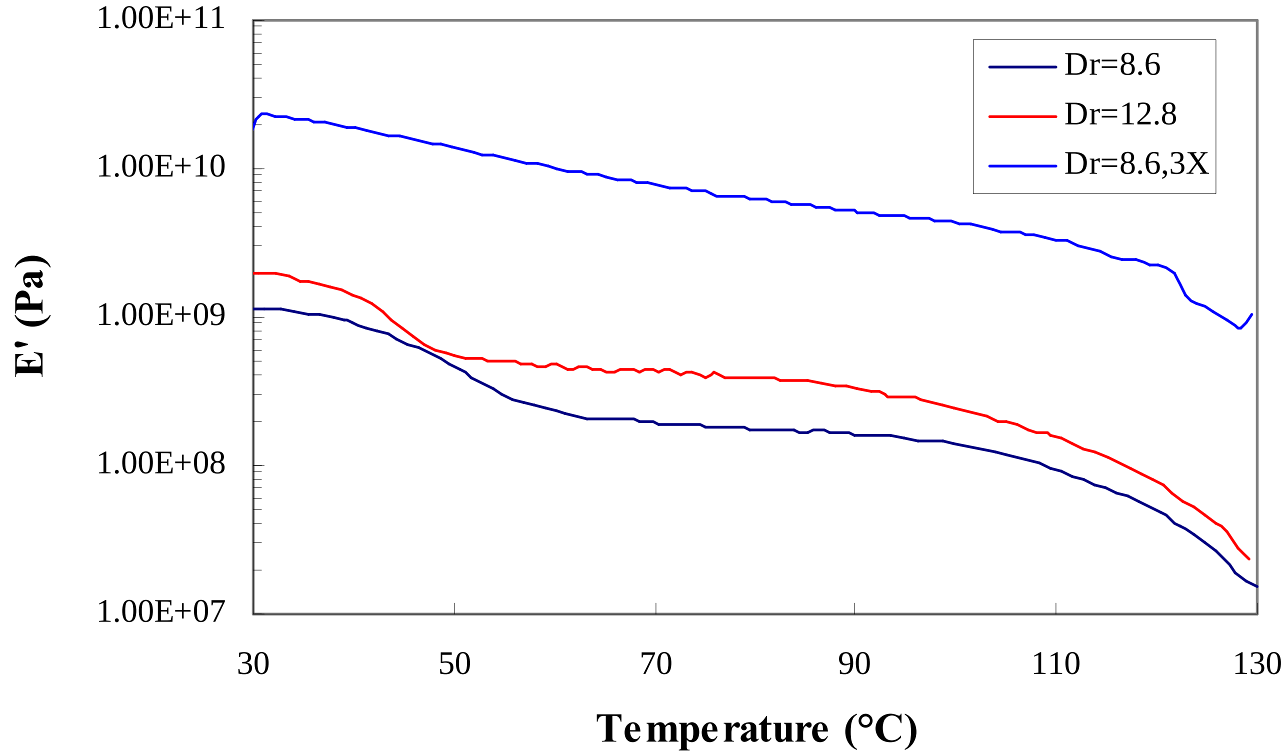

- X172 films at DR= 8.6 and 12.8, L = 5cm, T_{die} = 200 °C
- The sample with DR = 8.6 is uniaxially stretched (3X)
- Increasing modulus implies increasing orientation and crystallinity

Modeling

- **Continuity and Momentum eqns. (Thin film approximation)**

$$\nabla \cdot (d \underline{v}) = 0 , \nabla \cdot (d \underline{\underline{\sigma}}) = 0$$

$$d = d(x , y), \underline{v} = \underline{v}(x , y)$$

$$\underline{\underline{\sigma}} = p \underline{\underline{I}} + \underline{\underline{\tau}} = p \underline{\underline{I}} + \underline{\underline{\tau}}_s + \underline{\underline{\tau}}_p$$

  - $\underline{\underline{\sigma}}$ **is a plane stress tensor due to the thin film approximation**
  - **Stress related to deformation using Giesekus model**

$$\tau + \lambda_1 \tau_{(1)} - a \frac{\lambda_1}{\eta_0} \{ \tau \cdot \tau \} - a \lambda_2 \{ \dot{\gamma} \cdot \tau + \tau \cdot \dot{\gamma} \} = -\eta_0 \left[\dot{\gamma} + \lambda_2 \gamma_{(2)} - a \frac{\lambda_2^2}{\lambda_1} \{ \cdot \dot{\gamma} \cdot \dot{\gamma} \} \right]$$

- **Energy equation** $\rho C_p h \underline{v} \cdot \nabla T + 2 h_{tot} \left(T - T_{air} \right) = \rho h \Delta H_c \underline{v} \cdot \nabla X_c$

$$k(T) = K_{max} \ exp \left[- 4 \ln 2 \left(\frac{\left(T - T_{max} \right)^2}{D^2} \right) \right]$$

Model Calibration

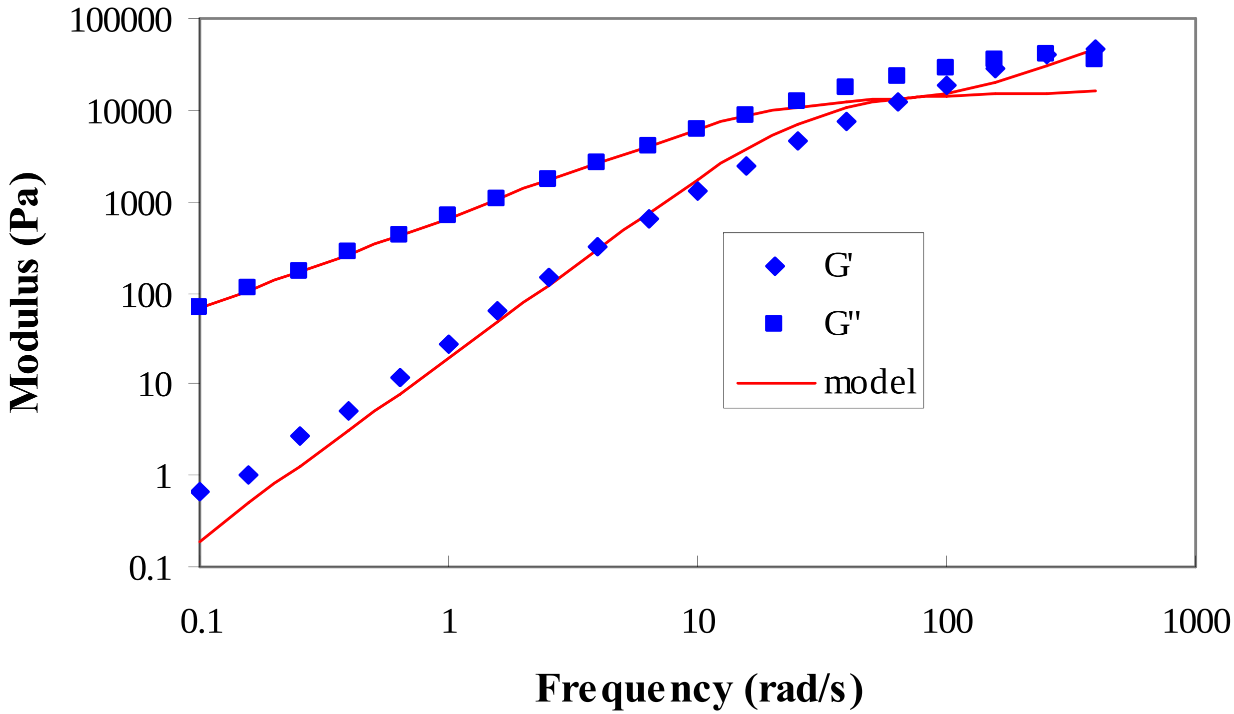

- **X172, 200 °C Giesekus fits**
- **Single mode model**
- **Determine** η_0, λ_1 , λ_2

Model Calibration

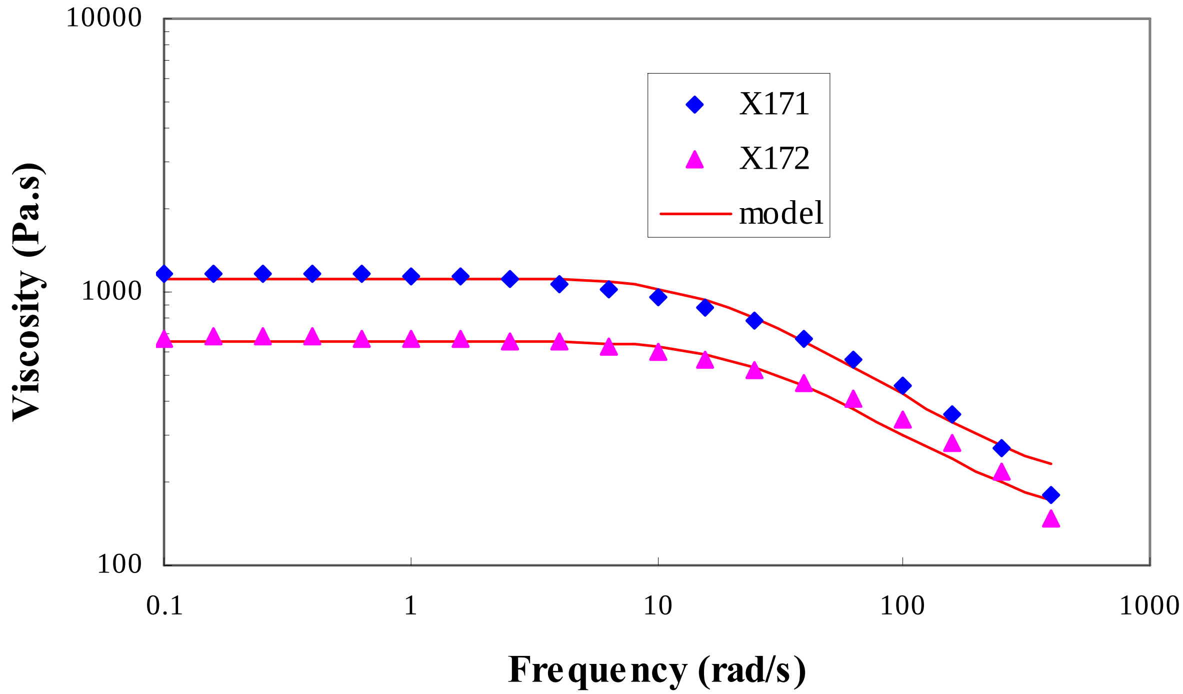

- **X171 and X172, 200 °C Giesekus fits**
- **Determine** α

Experiment vs. Model (Width Profile)

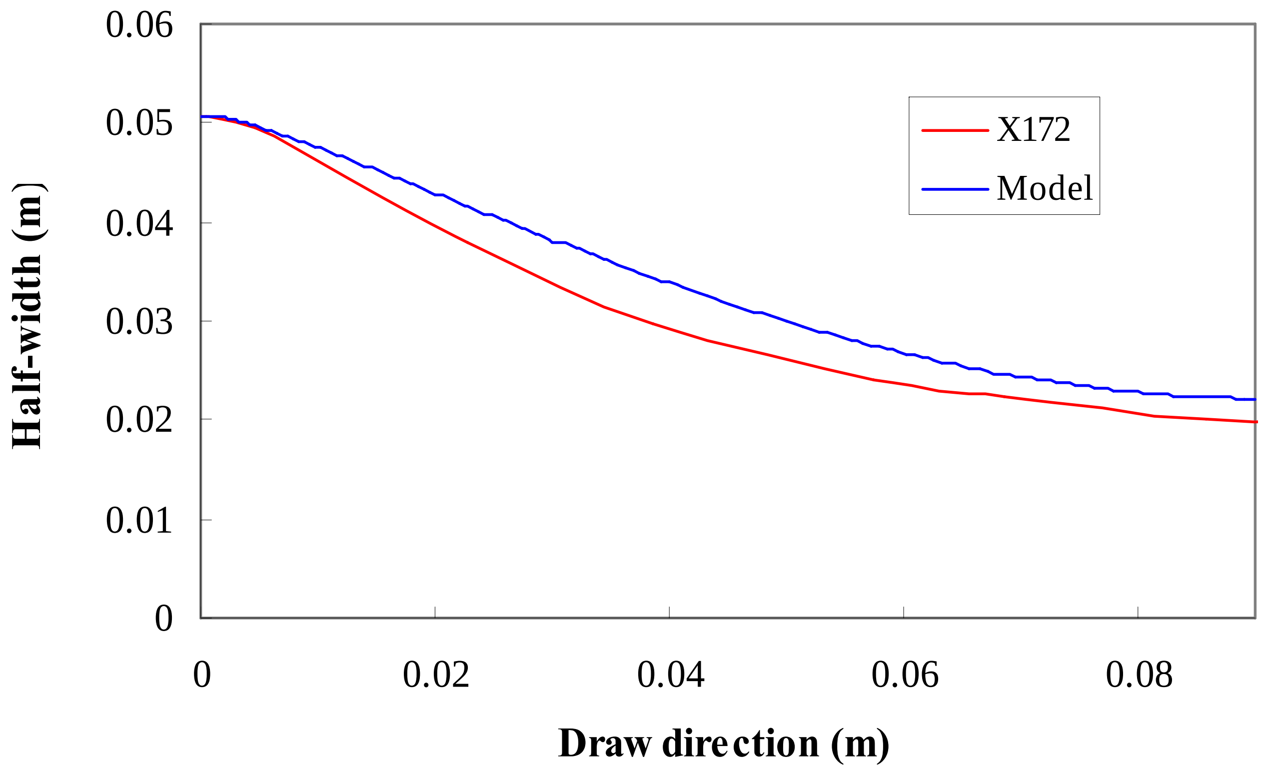

- **X172, T_{die} = 220 °C, L = 9 cm, DR = 8.6**
- **Model under-predicts the neck-in**
- **May be due to approximations**

Experiment vs. Model (Centerline Temperature)

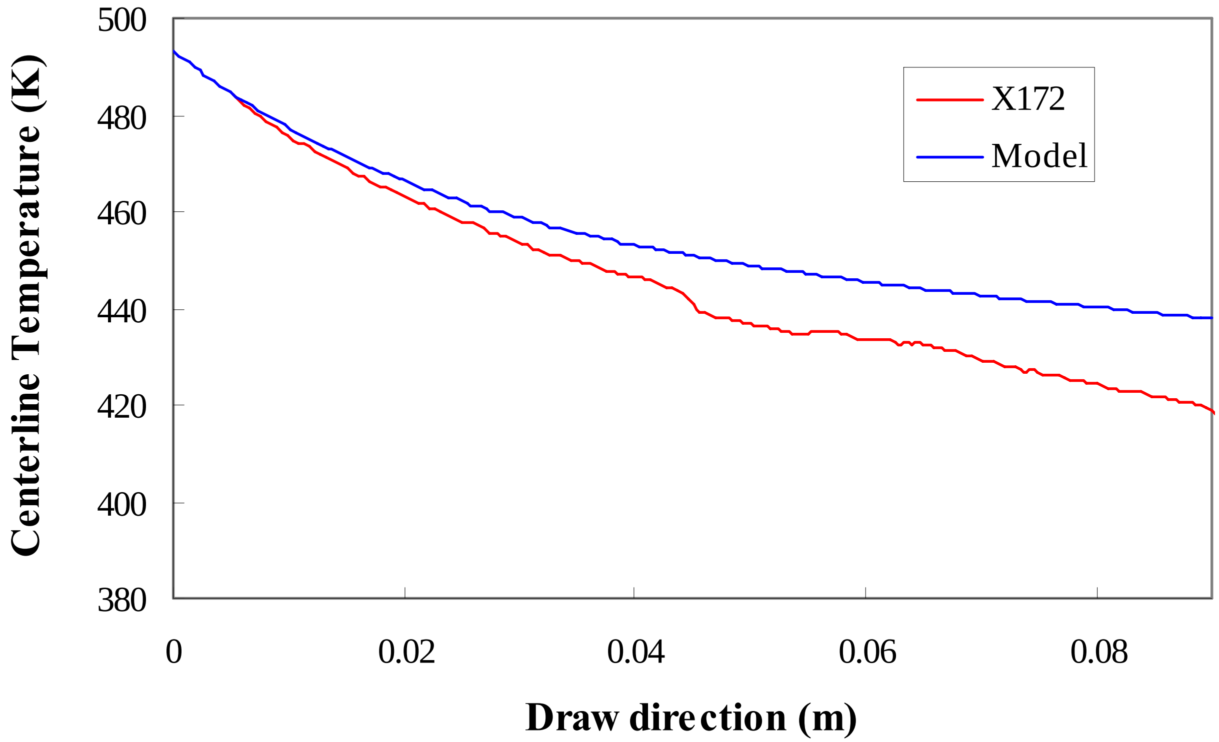

- **X172, T_{die} = 220 °C, L = 9 cm, DR = 8.6**
- **Model under-predicts the temperature drop**
- **May be due to model parameters and measurement technique**

Experiment vs. Model (Centerline Velocity)

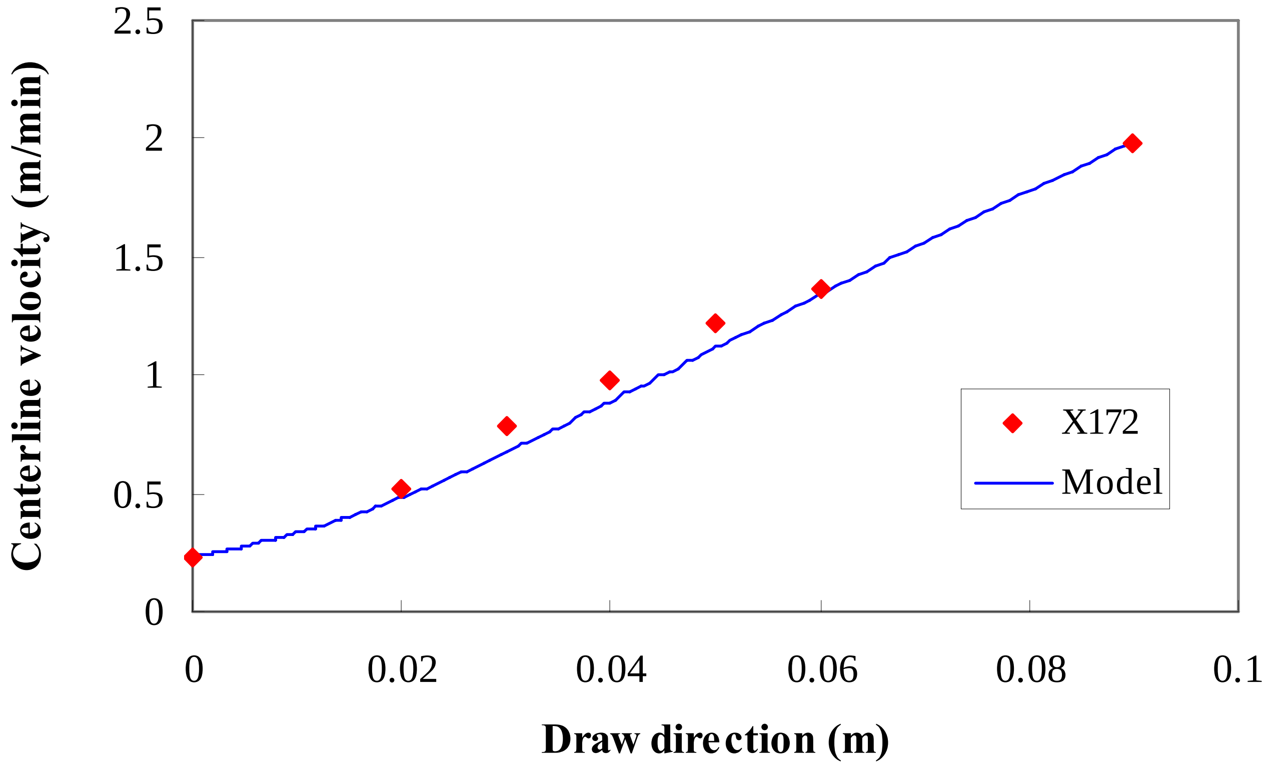

- X172, T_{die} = 220 °C, L = 9 cm, DR = 8.6
- Model gives better predictions for the velocity profile

Conclusions

- **Current work has focused on obtaining on-line velocity, temperature and width profiles in the web**
  - **Velocity and strain rate increase with increasing distance at high DR. At low DR the strain rate shows a maximum and then begins to decrease as the chill roll is approached.**
  - **Transverse velocity decreases from film edge to centerline.**
  - **Film temperatures decrease with increasing distance from the die**
  - **Film cools more rapidly with increasing draw ratio and increasing polymer viscosity**
  - **Die temperature, air-gap length and material properties impact neck-in, at a constant draw ratio**
  - **Coupling between process kinematics and thermodynamics due to temperature dependence of fluid viscosity**
- **Room for improvement on model predictions**

Acknowledgements

- **Center for Advanced Engineering Fibers and Films at Clemson University**
- **ERC program of the National Science Foundation (Award No. EEC-9731680) for financial support of this work.**
- **Dr. Christopher Cox, Dr. James B. von Oehsen, Scott Pearson**

Questions

PRESENTED BY
Kenneth Aniunoh
Center for Advanced Engineering Fibers and Films
Clemson University
kaniuno@clemson.edu

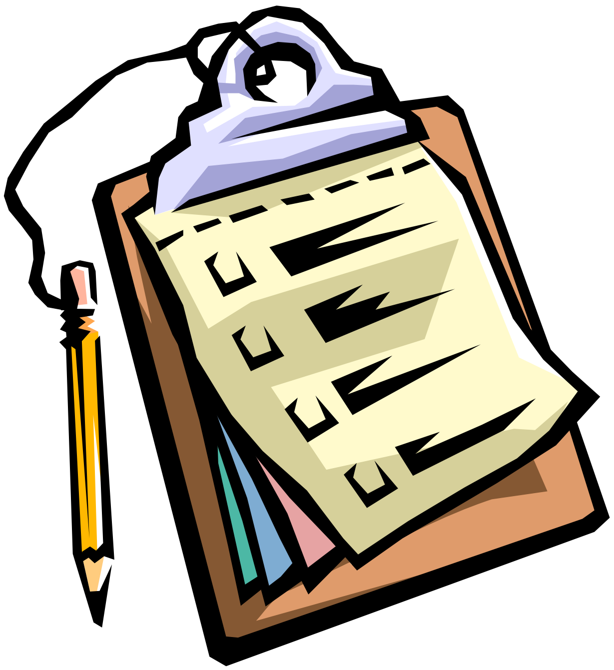

Please remember to turn in your evaluation sheet...